Computational Methods for Generalised Continua

René de Borst*

* School of Engineering, University of Glasgow, Glasgow, UK

Abstract Standard continuum models do not incorporate an internal length scale, and therefore suffer from excessive mesh dependence when strain-softening models are used in numerical analyses. In this contribution this phenomenon will be analysed and remedied through the use of higher-order continua. To enable an efficient and robust implementation algorithms based on damage and on plasticity theories will be described for higher-order gradient models and for a Cosserat continuum.

1 Introduction

Localisation of deformation refers to the emergence of narrow regions in a structure where all further deformation tends to concentrate, in spite of the fact that the external actions continue to follow a monotonic loading programme. The remaining parts of the structure usually unload and behave in an almost rigid manner. The phenomenon has a detrimental effect on the integrity of the structure and often acts as a direct precursor to structural failure. It is observed for a wide range of materials, including rocks, concrete, soils, metals, alloys and polymers, although the scale of localisation phenomena in the various materials may differ by some orders of magnitude: the band width is typically less than a millimeter in metals and several meters for crestal faults in rocks.

In this contribution we address the fundamental issue of developing (higher-order) continuum models that admit localisation of deformation while preserving well-posedness of the rate boundary value problem. In a standard (Boltzmann) continuum well-posedness is normally lost when the homogenised constitutive relation exhibits a descending branch, which is commonly referred to as strain softening.

A part of this contribution is hence devoted to uniqueness and stability issues of non-linear boundary value problems in standard continua. Emphasis is placed on the critical conditions which entail a change of type

H. Altenbach, V. A. Eremeyev (Eds.), *Generalized Continua from the Theory to Engineering Applications*, DOI 10.1007/978-3-7091-1371-4_7, © CISM, Udine 2013

of the differential equation, and the consequences of such a change for the discretisation sensitivity of computations. Subsequently, we discuss simple enhancements of the standard continuum theory within the framework of damage theory and of plasticity theory. Our aim is to obtain an enhanced continuum formulation that does not exhibit a change of type of the differential equation and therefore, does not suffer from excessive mesh sensitivity when strain softening occurs.

For large-scale applications of such higher-order continuum methods it is pivotal that the damage and plasticity models utilised are cast in an algorithmic framework that is robust and efficient. For this reason a major part of this contribution is devoted to the description of such algorithms.

2 Isotropic Elasticity-Based Damage

The basic structure of constitutive models that are set up in the spirit of damage mechanics is simple. We have a total stress-strain relation (Lemaitre and Chaboche, 1990):

$$\boldsymbol{\sigma} = \mathbf{D}^{\mathrm{s}}(\omega, \boldsymbol{\omega}, \boldsymbol{\Omega}) : \boldsymbol{\epsilon} \tag{1}$$

where $\boldsymbol{\sigma}$ is the stress tensor, $\boldsymbol{\epsilon}$ is the strain tensor and $\mathbf{D}^{\mathrm{s}}$ is a secant, fourth-order stiffness tensor, which can depend on a number of internal variables, like scalar-valued variables ω, second-order tensors $\boldsymbol{\omega}$ and fourth-order tensors $\boldsymbol{\Omega}$. Equation (1) differs from non-linear elasticity in the sense that a history dependence is incorporated via a loading-unloading function f. The theory is completed by specifying the appropriate (material-dependent) evolution equations for the internal variables.

For isotropic damage evolution, the secant stiffness tensor of Eq. (1) becomes (in matrix format):

$$\mathbf{D}^{\mathrm{s}} = \frac{E^{\mathrm{s}}}{(1+\nu^{\mathrm{s}})(1-2\nu^{\mathrm{s}})} \begin{bmatrix} 1-\nu^{\mathrm{s}} & \nu^{\mathrm{s}} & \nu^{\mathrm{s}} & 0 & 0 & 0 \\ \nu^{\mathrm{s}} & 1-\nu^{\mathrm{s}} & \nu^{\mathrm{s}} & 0 & 0 & 0 \\ \nu^{\mathrm{s}} & \nu^{\mathrm{s}} & 1-\nu^{\mathrm{s}} & 0 & 0 & 0 \\ 0 & 0 & 0 & \frac{1-2\nu^{\mathrm{s}}}{2} & 0 & 0 \\ 0 & 0 & 0 & 0 & \frac{1-2\nu^{\mathrm{s}}}{2} & 0 \\ 0 & 0 & 0 & 0 & 0 & \frac{1-2\nu^{\mathrm{s}}}{2} \end{bmatrix} \tag{2}$$

with $E^{\mathrm{s}} = E(1-\omega_1)$ the secant stiffness modulus, and $\nu^{\mathrm{s}} = \nu(1-\omega_2)$ the secant value of Poisson's ratio. The scalar-valued damage variables ω_1 and ω_2 grow from zero to one at complete damage. A further simplification can be achieved if it is assumed that Poisson's ratio remains constant during the damage process, which is equivalent to the assumption that the secant shear stiffness and bulk moduli degrade in the same manner during damage

evolution. Equation (2) then simplifies to:

$$\mathbf{D}^{\mathrm{s}} = (1-\omega)\mathbf{D}^{\mathrm{e}} \tag{3}$$

with ω the single damage variable.

The total stress-strain relation (3) is complemented by a damage loading function f, which reads:

$$f = f(\tilde{\epsilon}, \tilde{\sigma}, \kappa) \tag{4}$$

with $\tilde{\epsilon}$ and $\tilde{\sigma}$ scalar-valued functions of the strain and stress tensors, respectively, and κ the internal variable. The internal variable κ starts at an initial level κ_i and is updated by the requirement that during damage growth $f = 0$, whereas at unloading $f < 0$ and $\dot{\kappa} = 0$. Damage growth occurs according to an evolution law such that $\omega = \omega(\kappa)$, which can be determined from a uniaxial test. The loading-unloading conditions of inelastic constitutive models are often formalised using the Karush-Kuhn-Tucker conditions:

$$f \leq 0 \quad , \quad \dot{\kappa} \geq 0 \quad , \quad f\dot{\kappa} = 0 \tag{5}$$

We here limit the treatment to the case that the damage loading function does not depend on $\tilde{\sigma}$. For such a strain-based, or elasticity-based, damage model we have:

$$f(\tilde{\epsilon}, \kappa) = \tilde{\epsilon} - \kappa \tag{6}$$

For metals a common choice for $\tilde{\epsilon}$ is the energy measure:

$$\tilde{\epsilon} = \frac{1}{2}\boldsymbol{\epsilon} : \mathbf{D}^{\mathrm{e}} : \boldsymbol{\epsilon} \tag{7}$$

Equation (7) is less convenient in the sense that it does not reduce to the uniaxial strain for uniaxial stressing. For this reason it is sometimes replaced by the modified expression

$$\tilde{\epsilon} = \sqrt{\frac{1}{E}\,\boldsymbol{\epsilon} : \mathbf{D}^{\mathrm{e}} : \boldsymbol{\epsilon}} \tag{8}$$

Expression (8) is represented graphically in the principal strain space for plane-stress conditions in Figure 1(a). In this figure, a scaling has been applied such that $\tilde{\epsilon} = 1$, while $\nu = 0.2$. The dashed lines are uniaxial stress paths.

The above energy release rate definition for $\tilde{\epsilon}$ gives equal weights to tensile and compressive strain components, which makes it unsuitable to describe the mechanical behaviour of quasi-brittle materials like concrete,

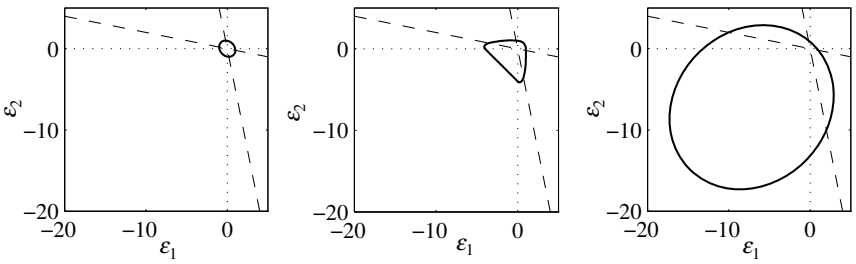

Figure 1. Contour plots for $\tilde{\epsilon}$ for (a) the energy-based concept, (b) the Mazars definition (Mazars and Pijaudier-Cabot, 1989) and (c) the modified Von Mises definition for $k = 10$

rock and ceramics. To remedy this deficiency, Mazars and Pijaudier-Cabot (1989) have suggested the definition

$$\tilde{\epsilon} = \sqrt{\sum_{i=1}^{3} (< \epsilon_i >)^2} \tag{9}$$

with ϵ_i the principal strains, with $< \cdot >$ the MacAulay brackets defined such that $< \epsilon_i >= \epsilon_i$ if $\epsilon_i > 0$ and $< \epsilon_i >= 0$ otherwise. A contour plot for $\tilde{\epsilon} = 1$ is given in Figure 1(b). A third definition for the equivalent strain $\tilde{\epsilon}$ has been proposed by de Vree et al. (1995). This proposition, which has been named a Modified von Mises definition, is given by

$$\tilde{\epsilon} = \frac{k-1}{2k(1-\nu)} I_1^{\epsilon} + \frac{1}{2k} \sqrt{\frac{(k-1)^2}{(1-2\nu)^2} (I_1^{\epsilon})^2 + \frac{12k}{(1+\nu)^2} J_2^{\epsilon}} \tag{10}$$

with I_1^{ϵ} the first invariant of the strain tensor and J_2^{ϵ} the second invariant of the deviatoric strain tensor. The parameter k governs the sensitivity to the compressive strain components relative to the tensile strain components. The definition of $\tilde{\epsilon}$ is such that a compressive uniaxial stress $k\sigma$ has the same effect as a uniaxial tensile stress σ. k is therefore normally set equal to the ratio of the compressive uniaxial strength and the tensile uniaxial strength. A graphical representation of the Modified von Mises definition is given in Figure 1(c).

From a computational point of view the above elasticity-based damage model is cast easily into a simple and robust algorithm. Indeed, in a displacement-based finite element formulation we can directly compute the strains from the given nodal displacements. The equivalent strain follows

in a straightforward fashion, since $\tilde{\epsilon} = \tilde{\epsilon}(\boldsymbol{\epsilon})$. After evaluation of the damage loading function, Eq. (6), the damage variable ω can be updated, and the new value for the stress tensor can be computed directly. The simple structure of the algorithm, see Box 1 for details, is due to the fact that the stress-strain relation of Eq. (1) is a total stress-strain relation, in the sense that there exists a bijective relation for unloading, and a surjective, but non-injective relation between the stress and strain tensors for loading.

Box 1. Algorithm for a isotropic elasticity-based damage model.

1. Compute the strain increment: $\Delta\boldsymbol{\epsilon}_{j+1}$
2. Update the total strain: $\boldsymbol{\epsilon}_{j+1} = \boldsymbol{\epsilon}_0 + \Delta\boldsymbol{\epsilon}_{j+1}$
3. Compute the equivalent strain: $\tilde{\epsilon}_{j+1} = \tilde{\epsilon}(\boldsymbol{\epsilon}_{j+1})$
4. Evaluate the damage loading function: $f = \tilde{\epsilon}_{j+1} - \kappa_0$

   if $f \geq 0$, $\kappa_{j+1} = \tilde{\epsilon}_{j+1}$

   else $\kappa_{j+1} = \kappa_0$
5. Update the damage variable: $\omega_{j+1} = \omega(\kappa_{j+1})$
6. Compute the new stresses: $\boldsymbol{\sigma}_{j+1} = (1 - \omega_{j+1})\mathbf{D}^{\mathrm{e}} : \boldsymbol{\epsilon}_{j+1}$

The algorithm described above evaluates the stress from a given strain. To arrive at a computationally efficient procedure that utilises a Newton-Raphson method, it must be complemented by a tangential stiffness tensor, which is derived by a consistent linearisation of the stress-strain relation. Differentiating Eq. (3) gives:

$$\dot{\boldsymbol{\sigma}} = (1 - \omega)\mathbf{D}^{\mathrm{e}} : \dot{\boldsymbol{\epsilon}} - \dot{\omega}\mathbf{D}^{\mathrm{e}} : \boldsymbol{\epsilon} \tag{11}$$

Since $\omega = \omega(\kappa)$, and because the internal variable κ depends on the equivalent strain via $\tilde{\epsilon}$ and the loading function (6), we obtain:

$$\dot{\omega} = \frac{\partial\omega}{\partial\kappa}\frac{\partial\kappa}{\partial\tilde{\epsilon}}\dot{\tilde{\epsilon}} \tag{12}$$

where $\partial\kappa/\partial\tilde{\epsilon} \equiv 1$ for loading and $\partial\kappa/\partial\tilde{\epsilon} \equiv 0$ for unloading. Considering the dependence $\tilde{\epsilon} = \tilde{\epsilon}(\boldsymbol{\epsilon})$, we can elaborate this relation as:

$$\dot{\omega} = \frac{\partial\omega}{\partial\kappa}\frac{\partial\kappa}{\partial\tilde{\epsilon}}\frac{\partial\tilde{\epsilon}}{\partial\boldsymbol{\epsilon}} : \dot{\boldsymbol{\epsilon}} \tag{13}$$

Substitution of Eq. (13) into the expression for the stress rate yields:

$$\dot{\boldsymbol{\sigma}} = \left((1-\omega)\mathbf{D}^{\mathrm{e}} - \frac{\partial \omega}{\partial \kappa}\frac{\partial \kappa}{\partial \tilde{\epsilon}}(\mathbf{D}^{\mathrm{e}} : \boldsymbol{\epsilon}) \otimes \frac{\partial \tilde{\epsilon}}{\partial \boldsymbol{\epsilon}} \right) : \dot{\boldsymbol{\epsilon}} \tag{14}$$

For unloading the second term in Eq. (14) cancels and we retrieve the secant stiffness matrix $(1-\omega)\mathbf{D}^{\mathrm{e}}$ as the tangential stiffness matrix for unloading. It is finally noted, cf. Simo and Ju (1987), that the tangential stiffness matrix as defined in (14) is generally non-symmetric. For the special choice that the equivalent strain is given by Eq. (7), symmetry is restored, since then

$$\dot{\boldsymbol{\sigma}} = \left((1-\omega)\mathbf{D}^{\mathrm{e}} - \frac{\partial \omega}{\partial \kappa}\frac{\partial \kappa}{\partial \tilde{\epsilon}}(\mathbf{D}^{\mathrm{e}} : \boldsymbol{\epsilon}) \otimes (\mathbf{D}^{\mathrm{e}} : \boldsymbol{\epsilon}) \right) : \dot{\boldsymbol{\epsilon}} \tag{15}$$

3 Stability, Ellipticity, and Mesh Sensitivity

A fundamental problem of incorporating damage evolution in standard continuum models is the inherent mesh sensitivity that occurs after reaching a certain damage level. This mesh sensitivity goes beyond the standard discretisation sensitivity of numerical approximation methods for partial differential equations and is not related to deficiencies in the discretisation methods. Instead, the underlying reason for this mesh sensitivity is a local change in character of the governing partial differential equations. This local change of character of the governing set of partial differential equations leads to a loss of well-posedness of the initial boundary value problem and results in an infinite number of possible solutions. After discretisation, a finite number of solutions results. For a finer discretisation, the number of solutions increases, which explains the observed mesh sensitivity.

Since the observed mesh sensitivity is of a fundamental nature, we shall first discuss some basic notions regarding stability and ellipticity. Subsequently, we elucidate the mathematical concepts by simple examples regarding mesh sensitivity.

3.1 Stability and Ellipticity

At the continuum level stable material behaviour is usually defined as the scalar product of the stress rate $\dot{\boldsymbol{\sigma}}$ and the strain rate $\dot{\boldsymbol{\epsilon}}$ being positive (Hill, 1958; Maier and Hueckel, 1979):

$$\dot{\boldsymbol{\epsilon}} : \dot{\boldsymbol{\sigma}} > 0 \tag{16}$$

although it can be linked in a rigorous manner to Lyapunov's mathematical definition of stability only for elastic materials (Koiter, 1969). In Eq. (16)

restriction is made to geometrical linearity. Extension to geometrical non-linearity is straightforward by replacing $\dot{\boldsymbol{\sigma}}$ by the rate of the First Piola-Kirchhoff stress tensor and $\dot{\boldsymbol{\epsilon}}$ by the velocity gradient. Evidently, the scalar product of Eq. (16) becomes negative when, in a uniaxial tension or compression test, the slope of the homogenised axial stress-axial strain curve is negative. This phenomenon is named strain softening and is not restricted to a damage mechanics framework, but can also occur in plasticity.

There is a class of material instabilities that can cause the scalar product of stress rate and strain rate to become negative without the occurrence of strain softening in the sense as defined above. These instabilities can arise when the predominant load-carrying mechanism of the material is due to frictional effects such as in sands, rock joints and in pre-cracked concrete. At a phenomenological level such material behaviour typically results in constitutive models which, in a multiaxial context, have a non-symmetric relation between the stress-rate tensor and the strain-rate tensor, e.g. as in Eq. (14), unless a special choice is made for the equivalent strain $\tilde{\epsilon}$. This lack of symmetry is sufficient to cause loss of material stability, even if the slope of the axial stress-strain curve is still rising (Rudnicki and Rice, 1974).

In the above discussion, the terminology 'homogenised' has been used. Here, we refer to the fact that initial flaws and boundary conditions inevitably induce an inhomogeneous stress state in a specimen. During progressive failure of a specimen these flaws and local stress concentrations cause strongly inhomogeneous deformations of the specimen. The procedure that is normally utilised to derive stress-strain relations, i.e. dividing the force by the virgin load-carrying area and dividing the displacement of the end of the specimen by the original length so as to obtain stress and strain, respectively, then no longer reflects what happens at a lower length scale and loses physical significance.

Limiting the discussion to incrementally-linear stress-strain relations, that is the relation between the stress rate $\dot{\boldsymbol{\sigma}}$ and the strain rate $\dot{\boldsymbol{\epsilon}}$ can be written as

$$\dot{\boldsymbol{\sigma}} = \mathbf{D} : \dot{\boldsymbol{\epsilon}} \tag{17}$$

with $\mathbf{D}$ the material tangential stiffness tensor, inequality (16) can be reformulated as

$$\dot{\boldsymbol{\epsilon}} : \mathbf{D} : \dot{\boldsymbol{\epsilon}} > 0 \tag{18}$$

The limiting case that the inequality (18) is replaced by an equality, marks the onset of unstable material behaviour. Mathematically, this is expressed by the loss of positive definiteness of the material tangential stiffness tensor $\mathbf{D}$:

$$\det(\mathbf{D}^{\mathrm{sym}}) = 0 \tag{19}$$

where the superscript *sym* denotes a symmetrised operator. Material instability can lead to structural instability. For a structure that occupies a volume V, Hill's definition (Hill, 1958) guarantees structural stability if

$$\int_V \dot{\boldsymbol{\epsilon}} : \dot{\boldsymbol{\sigma}} \, \mathrm{d}V > 0 \tag{20}$$

for all kinematically admissible $\dot{\boldsymbol{\epsilon}}$. Obviously, violation of inequality (16), i.e. loss of material stability, can lead to violation of Eq. (20), thus opening the possibility of structural instability. Accordingly, the existence of material instabilities, such as strain softening, can lead to structural instability, even in the absence of geometrically destabilising terms. Of course, there exist many cases where material instabilities and geometrical terms interact and are both (partly) responsible for structural instability.

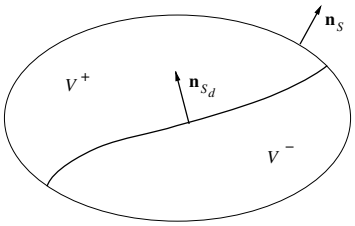

Figure 2. Body composed of continuous displacement fields at each side of the discontinuity S_d

Yet, the occurrence of unstable material behaviour does not explain the frequently observed discretisation-sensitive behaviour of computations of such solids. Indeed, a crucial consequence of the loss of positive definiteness of the material tangential stiffness tensor $\mathbf{D}$ is that it can result in loss of ellipticity of the governing set of rate equations. Considering quasi-static loading conditions, the governing differential equations – equilibrium equations, kinematic equations and constitutive equations – normally have an elliptic character. Mathematically, this implies that discontinuities in the solution are not possible. Now suppose that within the given context of quasi-static loading conditions, a (possibly curved) plane emerges, say S_d (Figure 2), across which the solution can be discontinuous. The difference in the traction rate $\dot{\mathbf{t}}_d$ across this plane reads:

$$[\![\dot{\mathbf{t}}_d]\!] = \mathbf{n}_{S_d} \cdot [\![\dot{\boldsymbol{\sigma}}]\!] \tag{21}$$

with $\mathbf{n}_{S_d}$ the normal vector to the discontinuity S_d. Using the tangential

stress-strain relation defined in Eq. (17) we obtain

$$[\![\dot{\mathbf{t}}_d]\!] = \mathbf{n}_{S_d} \cdot \mathbf{D} : [\![\dot{\boldsymbol{\epsilon}}]\!] \tag{22}$$

where the assumption of a linear comparison solid (Hill, 1958) has been introduced, i.e. $\mathbf{D}$ is assumed to have the same value at both sides of the discontinuity S_d. A displacement field $\mathbf{u}$ that is crossed by a single discontinuity can be represented as:

$$\mathbf{u} = \bar{\mathbf{u}} + \mathcal{H}_{S_d}\tilde{\mathbf{u}} \tag{23}$$

with the Heaviside function $\mathcal{H}_{S_d}$ separating the continuous displacement fields $\bar{\mathbf{u}}$ and $\tilde{\mathbf{u}}$. The strain field is subsequently obtained by straightforward differentiation:

$$\boldsymbol{\epsilon} = \nabla^{\mathrm{sym}}\bar{\mathbf{u}} + \mathcal{H}_{S_d}\nabla^{\mathrm{sym}}\tilde{\mathbf{u}} + \delta_{S_d}(\tilde{\mathbf{u}} \otimes \mathbf{n}_{S_d})^{\mathrm{sym}} \tag{24}$$

where δ_{S_d} is the Dirac function placed at the discontinuity S_d. For a stationary discontinuity, so that there is no variation of the Heaviside function $\mathcal{H}_{S_d}$ and the Dirac function δ_{S_d}, the strain rate field follows by differentiation with respect to time:

$$\dot{\boldsymbol{\epsilon}} = \nabla^{\mathrm{sym}}\dot{\bar{\mathbf{u}}} + \mathcal{H}_{S_d}\nabla^{\mathrm{sym}}\dot{\tilde{\mathbf{u}}} + \delta_{S_d}(\dot{\tilde{\mathbf{u}}} \otimes \mathbf{n}_{S_d})^{\mathrm{sym}} \tag{25}$$

The difference in strain rate fields at S_d is proportional to the unbounded term at the interface:

$$[\![\dot{\boldsymbol{\epsilon}}]\!] = \zeta(\dot{\tilde{\mathbf{u}}} \otimes \mathbf{n}_{S_d})^{\mathrm{sym}} \tag{26}$$

also known as the Maxwell compatibility condition and ζ a non-zero scalar. Substitution into Eq. (22) gives:

$$[\![\dot{\mathbf{t}}_d]\!] = \zeta(\mathbf{n}_{S_d} \cdot \mathbf{D} \cdot \mathbf{n}_{S_d}) \cdot \dot{\tilde{\mathbf{u}}} \tag{27}$$

where the minor symmetry of the tangential stiffness tensor has been exploited. A non-trivial solution can exist if and only if the determinant of the acoustic tensor $\mathbf{A} = \mathbf{n}_{S_d} \cdot \mathbf{D} \cdot \mathbf{n}_{S_d}$ vanishes:

$$\det(\mathbf{n}_{S_d} \cdot \mathbf{D} \cdot \mathbf{n}_{S_d}) = 0 \tag{28}$$

Thus, if condition (28) is met, discontinuous solutions can emerge and loss of ellipticity of the governing differential equations occurs. It is noted that condition (28) is coincident with Hill's condition for the propagation of plane acceleration waves in solids (Hill, 1962). Analyses that aim at determining the load level at which the determinant of the acoustic tensor vanishes are

also denoted as discontinuous bifurcation analyses, cf. Vardoulakis and Sulem (1995).

Ellipticity is a necessary condition for well-posedness of the rate boundary value problem, in the sense that a finite number of linearly independent solutions are admitted, continuously depending on the data and not involving discontinuities, cf. Benallal et al. (1988). Loss of ellipticity therefore allows an infinite number of solutions to occur, including those which involve discontinuities. A numerical approximation method will try to capture the discontinuity as good as possible and resolve it in the smallest possible volume which the discretisation allows. Accordingly, mesh refinement will result in a smaller and smaller localisation volume, but obviously, a discontinuity cannot be represented exactly unless special approximation methods are used that can capture a discontinuity rigorously.

For small displacement gradients loss of material stability as expressed by Eq. (19) is a necessary condition for loss of ellipticity. We show this by substituting the strain field (26) into the condition for loss of material stability (18):

$$(\tilde{\mathbf{u}} \otimes \mathbf{n}_{S_d}) : \mathbf{D} : (\tilde{\mathbf{u}} \otimes \mathbf{n}_{S_d}) > 0 \tag{29}$$

The left-hand side of this inequality vanishes for arbitrary $\tilde{\mathbf{u}}$ if and only if

$$\det(\mathbf{n}_{S_d} \cdot \mathbf{D}^{\mathrm{sym}} \cdot \mathbf{n}_{S_d}) = 0 \tag{30}$$

Because the real-valued eigenspectrum of the acoustic tensor $\mathbf{A}$ is bounded by the minimum and maximum eigenvalues of $\mathbf{n}_{S_d} \cdot \mathbf{D}^{\mathrm{sym}} \cdot \mathbf{n}_{S_d}$, Eq. (30) is always met prior to satisfaction of Eq. (28). Since Eq. (30) can only be satisfied if material stability is lost, Eq. (19), it follows that loss of ellipticity can occur only after loss of material stability. However, when geometrically non-linear terms are included, ellipticity can be lost prior to loss of material stability. This, for instance, can occur at low, but positive values of the plastic hardening modulus, in situations where geometrically non-linear terms have a destabilising effect.

3.2 Mesh Sensitivity

Mesh sensitivity in a standard continuum equipped with a strain-softening stress-strain relation is conveniently demonstrated by the example of a simple bar loaded in uniaxial tension, Figure 3. Let the bar be divided into m elements. Prior to reaching the tensile strength f_t a linear relation is assumed between the normal stress σ and the normal strain ϵ:

$$\sigma = E\epsilon$$

After reaching the peak strength a descending slope is defined in this diagram through an affine transformation from the measured load-displacement curve. The result is given in Figure 4(a), where κ_u marks the point where the load-carrying capacity is exhausted. In the post-peak regime the constitutive model thus reads:

$$\sigma = f_t + h(\epsilon - \kappa_i) \tag{31}$$

where, evidently, in case of degrading materials, $h < 0$ and may be termed a softening modulus. For linear strain softening we have

$$h = -\frac{f_t}{\kappa_u - \kappa_i} \tag{32}$$

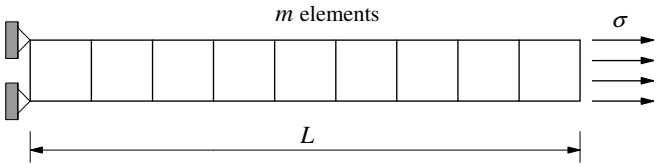

Figure 3. Bar with length L subjected to an axial tensile stress σ

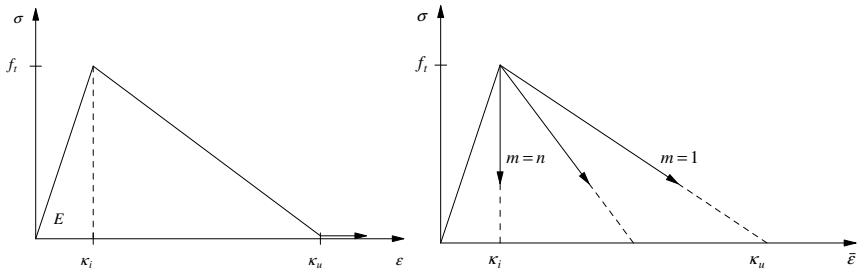

Figure 4. Left: Elastic-linear damaging material behaviour. Right: Response of an imperfect bar in terms of a stress-average strain curve

We next suppose that one element has a tensile strength that is marginally below that of the other $m-1$ elements. Upon reaching the tensile strength of this element, failure will occur. In the other, neighbouring elements the tensile strength is not exceeded and they will unload elastically. Beyond the peak strength the average strain in the bar is thus given by:

$$\bar{\epsilon} = \frac{\sigma}{E} + \frac{E-h}{Eh}\frac{\sigma - f_t}{m} \tag{33}$$

Substitution of Eq. (32) for the softening modulus h and introduction of n as the ratio between the strain κ_u at which the residual load-carrying capacity is exhausted and the threshold damage level κ_i, $n = \kappa_u/\kappa_i$ and $h = -E/(n-1)$, gives

$$\bar{\epsilon} = \frac{\sigma}{E} + \frac{n(f_t - \sigma)}{mE} \tag{34}$$

This result has been plotted in Figure 4(b) for different values of m for given n. The computed post-peak curves do not seem to converge to a unique curve. In fact, they do, because the governing equations predict the failure mechanism to be a line crack with zero thickness. The numerical solution simply tries to capture this line crack, which results in localisation in one element, irrespective of the width of the element. The impact on the stress-average strain curve is obvious: For an infinite number of elements ($m \to \infty$) the post-peak curve doubles back on the original loading curve. A major problem is now that, since in continuum mechanics the constitutive model is phrased in terms of a stress-strain relation and not as a force-displacement relation, the energy that is dissipated tends to zero upon mesh refinement, simply because the volume in which the failure process occurs also becomes zero. From a physical point of view this is unacceptable.

4 Non-Local and Gradient Damage Models

4.1 Non-Local Damage Models

In a non-local generalisation the equivalent strain $\tilde{\epsilon}$ is normally replaced by a spatially averaged quantity in the damage loading function (Pijaudier-Cabot and Bažant, 1987):

$$f(\bar{\epsilon}, \kappa) = \bar{\epsilon} - \kappa \tag{35}$$

where the non-local strain $\bar{\epsilon}$ is computed from:

$$\bar{\epsilon}(\mathbf{x}) = \frac{1}{\Psi(\mathbf{x})} \int_V \psi(\mathbf{y}, \mathbf{x}) \tilde{\epsilon}(\mathbf{y}) \mathrm{d}V \quad , \quad \Psi(\mathbf{x}) = \int_V \psi(\mathbf{y}, \mathbf{x}) \mathrm{d}V \tag{36}$$

with $\psi(\mathbf{y}, \mathbf{x})$ a weight function. Often, the weight function ψ is assumed to be homogeneous and isotropic, so that it only depends on the norm $s = \parallel \mathbf{x} - \mathbf{y} \parallel$. In this formulation all the other relations remain local: the local stress-strain relation, Eq. (3), the loading-unloading conditions, Eqs. (5), and the dependence of the damage variable ω on the internal variable κ: $\omega = \omega(\kappa)$. As an alternative to Eq. (36), the locally defined internal variable κ can be replaced in the damage loading function f by a

spatially averaged quantity $\bar{\kappa}$:

$$\bar{\kappa}(\mathbf{x}) = \frac{1}{\Psi(\mathbf{x})} \int_V \psi(\mathbf{y}, \mathbf{x}) \kappa(\mathbf{y}) \mathrm{d}V \tag{37}$$

The fact that in elasticity-based damage models the stress can be computed directly from the given strain, enables that a straightforward algorithm can be set up for non-local damage models. For the non-local damage model defined by Eq. (36) the algorithm of Box 2 applies. Although conceptually straightforward, the tangential stiffness matrix entails some inconvenient properties. Due to the non-local character of the constitutive relation the tangential stiffness matrix is full, i.e. the bandedness is lost. The introduction of a cut-off on the averaging function partly remedies this disadvantage, but an increased band width will nevertheless result. Secondly, symmetry can be lost (Pijaudier-Cabot and Huerta, 1991).

Box 2. Algorithm for a non-local elasticity-based damage model.

1. Compute the strain increment: $\Delta\boldsymbol{\epsilon}_{j+1}$
2. Update the total strain: $\boldsymbol{\epsilon}_{j+1} = \boldsymbol{\epsilon}_j + \Delta\boldsymbol{\epsilon}_{j+1}$
3. Compute the equivalent strain: $\tilde{\epsilon}_{j+1} = \tilde{\epsilon}(\boldsymbol{\epsilon}_{j+1})$
4. Compute the non-local equivalent strain:
   $\bar{\epsilon}_{j+1}(\mathbf{x}) = \sum_i w_i \psi(\mathbf{y}_i, \mathbf{x}) \tilde{\epsilon}_{j+1}(\mathbf{y}_i) V_{\text{elem}}$
5. Evaluate the damage loading function: $f = \bar{\epsilon}_{j+1} - \kappa_0$
   if $f \geq 0$, $\kappa_{j+1} = \bar{\epsilon}_{j+1}$
   else $\kappa_{j+1} = \kappa_0$
6. Update the damage variable: $\omega_{j+1} = \omega(\kappa_{j+1})$
7. Compute the new stresses: $\boldsymbol{\sigma}_{j+1} = (1 - \omega_{j+1}) \mathbf{D}^{\mathrm{e}} : \boldsymbol{\epsilon}_{j+1}$

4.2 Gradient Damage Models

Non-local constitutive relations can be considered as a point of departure for constructing gradient models, although we wish to emphasise that the latter class of models can also be defined directly by supplying higher-order gradients in the damage loading function. Yet, we will follow the first-mentioned route to underline the connection between integral and differential type non-local models. This is done either by expanding the kernel

$\tilde{\epsilon}$ of the integral in Eq. (36) in a Taylor series, or by expanding of the internal variable κ in Eq. (37) in a Taylor series. We will first consider the expansion of $\tilde{\epsilon}$ and then we will do the same for κ. If we truncate after the second-order terms and carry out the integration implied in Eq. (36) under the assumption of isotropy, the following relation ensues:

$$\bar{\epsilon} = \tilde{\epsilon} + c\nabla^2\tilde{\epsilon} \tag{38}$$

where c is a gradient parameter of the dimension length squared. It can be related to the averaging volume and then becomes dependent on the precise form of the weight function ψ. For instance, for a one-dimensional continuum and taking

$$\psi(s) = \frac{1}{\sqrt{2\pi}l}\mathrm{e}^{-s^2/2\ell^2} \tag{39}$$

we obtain $c = 1/2\ell^2$. Here, we adopt the phenomenological view that $\ell = \sqrt{2c}$ reflects the internal length scale of the failure process which we wish to describe macroscopically.

Formulation (38), known as the explicit gradient damage model, has a disadvantage when applied in a finite element context, namely that it requires computation of second-order gradients of the local equivalent strain $\tilde{\epsilon}$. Since this quantity is a function of the strain tensor, and since the strain tensor involves first-order derivatives of the displacements, third-order derivatives of the displacements have to be computed, which would necessitate $\mathcal{C}^2$-continuity of the shape functions. To obviate this problem, Eq. (38) is differentiated twice and the result is substituted again into Eq. (38). Again neglecting fourth-order terms this leads to:

$$\bar{\epsilon} - c\nabla^2\bar{\epsilon} = \tilde{\epsilon} \tag{40}$$

In Peerlings et al. (2001) it has been shown that the implicit gradient damage model of Eq. (40) becomes formally identical to a fully non-local formulation for a specific choice of the weighting function ψ in Eq. (36), which underlines that this formulation has a truly non-local character, in contrast to the explicit gradient formulation of Eq. (38).

Higher-order continua require additional boundary conditions. With Eq. (40) governing the damage process, either the averaged equivalent strain $\bar{\epsilon}$ itself or its normal derivative must be specified on the boundary S of the body:

$$\bar{\epsilon} = \bar{\epsilon}_{\mathrm{s}} \quad \text{or} \quad \mathbf{n}_S \cdot \nabla\bar{\epsilon} = \bar{\epsilon}_{\mathrm{ns}} \tag{41}$$

In most example calculations in the literature the natural boundary condition $\mathbf{n}_S \cdot \nabla\bar{\epsilon} = 0$ has been adopted.

In a fashion similar to the derivation of the gradient damage models based on the averaging of the equivalent strain $\tilde{\epsilon}$, we can elaborate a gradient approximation of Eq. (37), i.e. by developing κ into a Taylor series. For an isotropic, infinite medium and truncating after the second term we have (de Borst et al., 1996):

$$\bar{\kappa} = \kappa + c\nabla^2\kappa \tag{42}$$

Since the weight functions for the different gradient formulations may be quite different, also the gradient parameter c may be very different for the various formulations. For instance, the gradient parameter c of Eq. (42) may differ considerably from those in Eqs. (38) or (40). The additional boundary conditions now apply to κ. Although formally similar to those of Eq. (41), namely

$$\kappa = \kappa_{\rm s} \quad \text{or} \quad \mathbf{n}_S \cdot \nabla\kappa = \kappa_{\rm ns} \tag{43}$$

they have a different character, since they apply to an internal variable instead of to a kinematic quantity, which seems somewhat suspect. On the other hand, the physical interpretation that can be given to the boundary condition $(43)_2$ is rather clear. Since the damage variable ω is a function of the internal variable κ, and therefore, the differential equation (42) and the boundary conditions (43) can be replaced by (de Borst et al., 1996):

$$\bar{\omega} = \omega + c\nabla^2\omega \tag{44}$$

where $\bar{\omega}$ is a spatially averaged damage field, similar to $\bar{\epsilon}$ or $\bar{\kappa}$, and the corresponding boundary conditions

$$\omega = \omega_{\rm s} \quad \text{or} \quad \mathbf{n}_S \cdot \nabla\omega = \omega_{\rm ns} \tag{45}$$

Equation $(45)_2$ with $\omega_{\rm ns} = 0$ can be identified as a condition of no damage flux through the boundary S of the body.

Numerical schemes for gradient-enhanced continua typically have the character of a coupled problem and depart from the weak form of the balance of momentum,

$$\int_V \delta\boldsymbol{\epsilon}^{\rm T}\boldsymbol{\sigma}{\rm d}V = \int_S \delta\mathbf{u}^{\rm T}\mathbf{t}{\rm d}S \tag{46}$$

and a weak form of the averaging equation, e.g. Eq. (40):

$$\int_V \delta\bar{\epsilon}\ (\bar{\epsilon} - c\nabla^2\bar{\epsilon} - \tilde{\epsilon}){\rm d}V = 0 \tag{47}$$

with $\delta\bar{\epsilon}$ the variational field of the non-local strain $\bar{\epsilon}$. Transforming Eq. (47), using the divergence theorem and the natural boundary condition $\mathbf{n}_S \cdot \nabla\bar{\epsilon} =$

0 yields:

$$\int_V (\delta\bar{\epsilon}\ \bar{\epsilon} + c\nabla\delta\bar{\epsilon}\cdot\nabla\bar{\epsilon})\mathrm{d}V = \int_V \delta\bar{\epsilon}\ \tilde{\epsilon}\mathrm{d}V \tag{48}$$

From Eq. (48) it is clear that in this formulation a $\mathcal{C}^0$-interpolation for $\bar{\epsilon}$ suffices. Accordingly, we can discretise the displacements $\mathbf{u}$ and the non-local strains

$$\mathbf{u} = \mathbf{H}\mathbf{a} \ \text{ and } \ \bar{\epsilon} = \bar{\mathbf{H}}\mathbf{e} \tag{49}$$

where $\mathbf{H}$ and $\bar{\mathbf{H}}$ contain $\mathcal{C}^0$-interpolation polynomials which can have a different order. Similarly, for the variations

$$\delta\mathbf{u} = \mathbf{H}\delta\mathbf{a} \ \text{ and } \ \delta\bar{\epsilon} = \bar{\mathbf{H}}\delta\mathbf{e} \tag{50}$$

Substitution into Eqs. (46), (48) and requiring that the result holds for arbitrary $(\delta\mathbf{a}, \delta\mathbf{e})$, yields the discrete format of the equilibrium equation:

$$\int_V \mathbf{B}^{\mathrm{T}}\boldsymbol{\sigma}\mathrm{d}V = \int_S \mathbf{H}^{\mathrm{T}}\mathbf{t}\mathrm{d}S \tag{51}$$

and of the averaging equation:

$$\int_V (\bar{\mathbf{H}}^{\mathrm{T}}\bar{\mathbf{H}} + c\bar{\mathbf{B}}^{\mathrm{T}}\bar{\mathbf{B}})\mathrm{d}V = \int_V \bar{\mathbf{H}}^{\mathrm{T}}\tilde{\boldsymbol{\epsilon}}\mathrm{d}V \tag{52}$$

where $\bar{\mathbf{B}}$ contains the spatial derivatives of $\bar{\mathbf{H}}$. An algorithm for computing the right-hand side of this model is given in Box 3.

Box 3. Algorithm for a second-order implicit gradient damage model.

1. Compute the strain increment: $\Delta\boldsymbol{\epsilon}_{j+1}$ and the non-local strain increment $\Delta\bar{\epsilon}_{j+1}$
2. Update the total strain: $\boldsymbol{\epsilon}_{j+1} = \boldsymbol{\epsilon}_j + \Delta\boldsymbol{\epsilon}_{j+1}$ and the non-local strain $\bar{\epsilon}_{j+1} = \bar{\epsilon}_j + \Delta\bar{\epsilon}_{j+1}$
3. Evaluate the damage loading function: $f = \bar{\epsilon}_{j+1} - \kappa_0$
   if $f \geq 0$, $\kappa_{j+1} = \bar{\epsilon}_{j+1}$
   else $\kappa_{j+1} = \kappa_0$
4. Update the damage variable: $\omega_{j+1} = \omega(\kappa_{j+1})$
5. Compute the new stresses: $\boldsymbol{\sigma}_{j+1} = (1 - \omega_{j+1})\mathbf{D}^{\mathrm{e}} : \boldsymbol{\epsilon}_{j+1}$

The tangential stiffness matrix needed for an iterative solution via the Newton-Raphson method reads (Peerlings et al., 1996):

$$\begin{bmatrix} \mathbf{K}_{\mathrm{aa}} & \mathbf{K}_{\mathrm{ae}} \\ \mathbf{K}_{\mathrm{ea}} & \mathbf{K}_{\mathrm{ee}} \end{bmatrix} \begin{pmatrix} \mathrm{d}\mathbf{a} \\ \mathrm{d}\mathbf{e} \end{pmatrix} = \begin{pmatrix} \mathbf{f}^{\mathrm{a}}_{\mathrm{ext}} - \mathbf{f}^{\mathrm{a}}_{\mathrm{int}} \\ \mathbf{f}^{\mathrm{e}}_{\mathrm{int}} - \mathbf{K}_{\mathrm{ee}}\mathbf{e} \end{pmatrix} \tag{53}$$

with $\mathbf{f}^{\mathrm{e}}_{\mathrm{int}}$ given by the right-hand side of Eq. (52). The stiffness matrices are given by:

$$\mathbf{K}_{\mathrm{aa}} = \int_V (1-\omega)\mathbf{B}^{\mathrm{T}}\mathbf{D}^{\mathrm{e}}\mathbf{B}\mathrm{d}V \tag{54}$$

$$\mathbf{K}_{\mathrm{ae}} = \int_V q\mathbf{B}^{\mathrm{T}}\mathbf{D}^{\mathrm{e}}\boldsymbol{\epsilon}\bar{\mathbf{H}}\mathrm{d}V \tag{55}$$

$$\mathbf{K}_{\mathrm{ea}} = \int_V \bar{\mathbf{H}}^{\mathrm{T}}\left(\frac{\partial\tilde{\epsilon}}{\partial\boldsymbol{\epsilon}}\right)\mathbf{B}\mathrm{d}V \tag{56}$$

$$\mathbf{K}_{\mathrm{ee}} = \int_V \left(\bar{\mathbf{H}}^{\mathrm{T}}\bar{\mathbf{H}} + c\bar{\mathbf{B}}^{\mathrm{T}}\bar{\mathbf{B}}\right)\mathrm{d}V \tag{57}$$

where $q = \partial\omega/\partial\kappa$ for loading and vanishes if otherwise. The expressions for $\mathbf{K}_{\mathrm{ae}}$ and $\mathbf{K}_{\mathrm{ea}}$ exhibit a non-symmetry. This non-symmetry is caused by the damage formalism and not by the gradient enhancement, cf. Eq. (14).

5 Cosserat Elasto-Plasticity

5.1 Cosserat Elasticity

In the present treatment we shall limit attention to two-dimensional, planar deformations. In that case, each material point in a micro-polar solid has two translational degrees-of-freedom, namely u_x and u_y and a rotational degree-of-freedom ω_z, the rotation axis of which is orthogonal to the x, y-plane. The normal strains are defined as in a standard continuum, but for the shear strains we have:

$$\epsilon_{xy} = \frac{\partial u_x}{\partial y} + \omega_z \tag{58}$$

and

$$\epsilon_{yx} = \frac{\partial u_y}{\partial x} - \omega_z \tag{59}$$

In addition to the normal strains and the shear strains, the Cosserat theory requires the introduction of micro-curvatures:

$$\kappa_{zx} = \frac{\partial \omega_z}{\partial x} \tag{60}$$

and

$$\kappa_{zy} = \frac{\partial \omega_z}{\partial y} \tag{61}$$

Anticipating the treatment for elasto-plasticity we will rather use the generalised curvatures $\kappa_{zx}\ell$ and $\kappa_{zy}\ell$, where ℓ is a material parameter with the dimension of length. It is this parameter which effectively sets the internal length scale in the continuum, and attains the role of a characteristic length scale.

The strain components introduced sofar may be assembled in a vector,

$$\boldsymbol{\epsilon} = (\epsilon_{xx}, \epsilon_{yy}, \epsilon_{zz}, \epsilon_{xy}, \epsilon_{yx}, \kappa_{zx}\ell, \kappa_{zy}\ell)^{\mathrm{T}} \tag{62}$$

Note that in addition to the strain components, also the normal strain in the z-direction, ϵ_{zz} has been included in the strain vector $\boldsymbol{\epsilon}$. This has been done because, although this strain component remains zero under plane strain conditions during the entire loading process, this is not necessarily the case for the elastic and plastic contributions of this strain component. Also, the normal stress σ_{zz}, which acts in the z-direction, may be non-zero, which necessitates inclusion of ϵ_{zz} and σ_{zz} in the stress-strain relation. It is furthermore noted that by multiplying the micro-curvatures κ_{zx} and κ_{zy} by the length parameter ℓ all the components of the strain vector $\boldsymbol{\epsilon}$ have the same dimension.

We now consider the statics of a Cosserat continuum. While the strain vector $\boldsymbol{\epsilon}$ is comprised of seven components for planar deformations, so is the stress vector $\boldsymbol{\sigma}$. As in a classical continuum we have the normal stresses σ_{xx}, σ_{yy} and σ_{zz}, and the shear stresses σ_{xy}, σ_{yx}. For the Cosserat continuum we also have to introduce stress quantities that are conjugate to the curvatures κ_{zx} and κ_{zy}, namely the couple stresses m_{zx} and m_{zy}. Dividing the couple stresses by the length parameter ℓ, we obtain a stress vector $\boldsymbol{\sigma}$ in which all the entries have the same dimension:

$$\boldsymbol{\sigma} = (\sigma_{xx}, \sigma_{yy}, \sigma_{zz}, \sigma_{xy}, \sigma_{yx}, m_{zx}/\ell, m_{zy}/\ell)^{\mathrm{T}} \tag{63}$$

Omitting body forces and body couples for sake of simplicity, translational equilibrium in the x and the y-directions, respectively, results in the usual balance of momentum:

$$\frac{\partial \sigma_{xx}}{\partial x} + \frac{\partial \sigma_{xy}}{\partial y} = 0$$

$$\frac{\partial \sigma_{yx}}{\partial x} + \frac{\partial \sigma_{yy}}{\partial y} = 0$$

which replicates the results obtained for a classical, non-polar continuum. However, for rotational equilibrium we find that:

$$\frac{\partial m_{zx}}{\partial x} + \frac{\partial m_{zy}}{\partial y} - (\sigma_{xy} - \sigma_{yx}) = 0 \tag{64}$$

which shows that the stress tensor is in general only symmetric – $\sigma_{xy} = \sigma_{yx}$ – if the couple-stresses m_{zx} and m_{zy} vanish, the so-called Boltzmann's Axiom.

Anticipating the treatment of Cosserat plasticity we decompose the strain vector into an elastic contribution $\boldsymbol{\epsilon}^{\mathrm{e}}$ and a plastic part $\boldsymbol{\epsilon}^{\mathrm{p}}$:

$$\boldsymbol{\epsilon} = \boldsymbol{\epsilon}^{\mathrm{e}} + \boldsymbol{\epsilon}^{\mathrm{p}} \tag{65}$$

while we assume that the elastic strains are linearly related to the stresses:

$$\boldsymbol{\sigma} = \mathbf{D}^{\mathrm{e}} : \boldsymbol{\epsilon}^{\mathrm{e}} \tag{66}$$

where $\mathbf{D}^{\mathrm{e}}$ is the stiffness matrix that contains the elastic moduli:

$$\mathbf{D}^{\mathrm{e}} = \begin{bmatrix} 2\mu c_1 & 2\mu c_2 & 2\mu c_2 & 0 & 0 & 0 & 0 \\ 2\mu c_2 & 2\mu c_1 & 2\mu c_2 & 0 & 0 & 0 & 0 \\ 2\mu c_2 & 2\mu c_2 & 2\mu c_1 & 0 & 0 & 0 & 0 \\ 0 & 0 & 0 & \mu + \mu_c & \mu - \mu_c & 0 & 0 \\ 0 & 0 & 0 & \mu - \mu_c & \mu + \mu_c & 0 & 0 \\ 0 & 0 & 0 & 0 & 0 & 2\mu & 0 \\ 0 & 0 & 0 & 0 & 0 & 0 & 2\mu \end{bmatrix} \tag{67}$$

with $c_1 = \frac{1-\nu}{1-2\nu}$ and $c_2 = \frac{\nu}{1-2\nu}$. The elastic constants μ and ν have the classical meaning of the shear modulus and Poisson's ratio, respectively. μ_c is an additional material constant, completing the total of four material constants, viz. μ, ν, ℓ and μ_c that are needed to describe the elastic behaviour of an isotropic Cosserat continuum under planar deformations. The coefficient two has been introduced in the terms D^{e}_{66} and D^{e}_{77} in order to arrive at a convenient form of the elasto-plastic constitutive equations. The total (bending) stiffness that sets the relation between the micro-curvatures and the couple stresses is basically determined by the value of the internal length scale ℓ. All the elastic stiffness moduli in $\mathbf{D}^{\mathrm{e}}$ have the same dimension. This is attributable to the fact that all components of the strain vector $\boldsymbol{\epsilon}$ and the stress vector $\boldsymbol{\sigma}$ have the same dimension.

5.2 Cosserat Plasticity

As an example we use a pressure-dependent J_2-flow theory (Drucker-Prager model). Accordingly, the yield function f can be written as

$$f(\boldsymbol{\sigma}, \gamma) = \sqrt{3J_2} + \alpha p - \bar{\sigma}(\gamma) \tag{68}$$

with $\bar{\sigma}$ a function of the hardening parameter γ and α a friction coefficient. $p = \frac{1}{3}(\sigma_{xx} + \sigma_{yy} + \sigma_{zz})$ and J_2 is the second invariant of the deviatoric stresses, which, for a micro-polar continuum, can be generalised as:

$$J_2 = a_1 \mathbf{s}^{\mathrm{T}} : \mathbf{s} + a_2 \mathbf{s} : \mathbf{s} + a_3 \mathbf{m} : \mathbf{m}/\ell^2 \tag{69}$$

where the summation convention with respect to repeated indices has been adopted. $\mathbf{s}$ is the deviatoric stress tensor and a_1, a_2 and a_3 are material parameters. In the absence of couple-stresses, i.e. $\mathbf{m} = \mathbf{0}$, $\mathbf{s} = \mathbf{s}^{\mathrm{T}}$, so that:

$$J_2 = a_1 \mathbf{s}^{\mathrm{T}} : \mathbf{s} + a_2 \mathbf{s} : \mathbf{s} \tag{70}$$

which implies that the constraint $a_1 + a_2 = \frac{1}{2}$ must be enforced to achieve that the classical expression for J_2 be retrieved. Introduction of the projetion matrix

$$\mathbf{P} = \begin{bmatrix} \frac{2}{3} & -\frac{1}{3} & -\frac{1}{3} & 0 & 0 & 0 & 0 \\ -\frac{1}{3} & \frac{2}{3} & -\frac{1}{3} & 0 & 0 & 0 & 0 \\ -\frac{1}{3} & -\frac{1}{3} & \frac{2}{3} & 0 & 0 & 0 & 0 \\ 0 & 0 & 0 & 2a_1 & 2a_2 & 0 & 0 \\ 0 & 0 & 0 & 2a_2 & 2a_1 & 0 & 0 \\ 0 & 0 & 0 & 0 & 0 & 2a_3 & 0 \\ 0 & 0 & 0 & 0 & 0 & 0 & 2a_3 \end{bmatrix} \tag{71}$$

and the projection vector:

$$\boldsymbol{\pi}^{\mathrm{T}} = \left(\frac{1}{3}, \frac{1}{3}, \frac{1}{3}, 0, 0, 0, 0 \right) \tag{72}$$

for planar deformations, enables a rewriting of the yield function in an appealingly compact format:

$$f(\boldsymbol{\sigma}, \gamma) = \sqrt{\frac{3}{2} \boldsymbol{\sigma}^{\mathrm{T}} \mathbf{P} \boldsymbol{\sigma}} + \alpha \boldsymbol{\pi}^{\mathrm{T}} \boldsymbol{\sigma} - \bar{\sigma}(\gamma) \tag{73}$$

A (non-associated) flow rule is now obtained in an identical fashion to that in a non-polar continuum by defining a resembling plastic potential function:

$$g(\boldsymbol{\sigma}, \gamma) = \sqrt{\frac{3}{2} \boldsymbol{\sigma}^{\mathrm{T}} \mathbf{P} \boldsymbol{\sigma}} + \beta \boldsymbol{\pi}^{\mathrm{T}} \boldsymbol{\sigma} - \bar{\sigma}(\gamma) \tag{74}$$

with β a dilatancy factor, from which the plastic strain rates can be derived:

$$\dot{\boldsymbol{\epsilon}}^{\mathrm{p}} = \dot{\lambda} \frac{\partial g}{\partial \boldsymbol{\sigma}} \tag{75}$$

with $\dot{\lambda}$ the plastic multiplier which, in analogy with standard plasticity theory, is determined from the consistency condition $\dot{f} = 0$. Substitution of the plastic potential for the Drucker-Prager plasticity model, Eq. (74), into the above expression for the plastic strain rate yields

$$\dot{\boldsymbol{\epsilon}}^{\mathrm{p}} = \dot{\lambda} \left(\frac{3\mathbf{P}\boldsymbol{\sigma}}{2\sqrt{\frac{3}{2}\boldsymbol{\sigma}^{\mathrm{T}}\mathbf{P}\boldsymbol{\sigma}}} + \beta\boldsymbol{\pi} \right) \tag{76}$$

It remains to identify the hardening parameter γ in a Cosserat continuum. For this purpose we recall the conventional strain-hardening hypothesis:

$$\dot{\gamma} = \sqrt{\frac{2}{3}\dot{\mathbf{e}}^{\mathrm{p}} : \dot{\mathbf{e}}^{\mathrm{p}}} \tag{77}$$

with $\dot{\mathbf{e}}^{\mathrm{p}}$ the deviatoric plastic strain-rate tensor. Since there are no couple-stress effects in uniaxial loading we require that any modification for a Cosserat continuum does not affect the behaviour for uniaxial loading. A possible generalisation is then:

$$\dot{\gamma} = \sqrt{b_1(\dot{\mathbf{e}}^{\mathrm{p}})^{\mathrm{T}} : \dot{\mathbf{e}}^{\mathrm{p}} + b_2\dot{\mathbf{e}}^{\mathrm{p}} : \dot{\mathbf{e}}^{\mathrm{p}} + b_3\dot{\boldsymbol{\kappa}}^{\mathrm{p}} : \dot{\boldsymbol{\kappa}}^{\mathrm{p}}/\ell^2} \tag{78}$$

with $b_1 + b_2 = \frac{2}{3}$ in order that definition the strain-hardening hypothesis in a non-polar solid be retrieved. Introduction of the matrix

$$\mathbf{Q} = \begin{bmatrix} \frac{2}{3} & -\frac{1}{3} & -\frac{1}{3} & 0 & 0 & 0 & 0 \\ -\frac{1}{3} & \frac{2}{3} & -\frac{1}{3} & 0 & 0 & 0 & 0 \\ -\frac{1}{3} & -\frac{1}{3} & \frac{2}{3} & 0 & 0 & 0 & 0 \\ 0 & 0 & 0 & \frac{3}{2}b_1 & \frac{3}{2}b_2 & 0 & 0 \\ 0 & 0 & 0 & \frac{3}{2}b_2 & \frac{3}{2}b_1 & 0 & 0 \\ 0 & 0 & 0 & 0 & 0 & \frac{3}{2}b_3 & 0 \\ 0 & 0 & 0 & 0 & 0 & 0 & \frac{3}{2}b_3 \end{bmatrix} \tag{79}$$

allows $\dot{\gamma}$ to be written as:

$$\dot{\gamma} = \sqrt{\frac{2}{3}(\dot{\boldsymbol{\epsilon}}^{\mathrm{p}})^{\mathrm{T}}\mathbf{Q}\dot{\boldsymbol{\epsilon}}^{\mathrm{p}}} \tag{80}$$

for planar deformations. We next substitute the flow rule, Eq. (76), into this expression. The result is given by:

$$\dot{\gamma} = \dot{\lambda}\sqrt{\frac{\boldsymbol{\sigma}^{\mathrm{T}}\mathbf{P}\mathbf{Q}\mathbf{P}\boldsymbol{\sigma}}{\boldsymbol{\sigma}^{\mathrm{T}}\mathbf{P}\boldsymbol{\sigma}}} \tag{81}$$

since $\dot{\lambda}$ and $\bar{\sigma}$ are non-negative, and $\mathbf{Q}\boldsymbol{\pi} = \mathbf{0}$. In line with a standard continuum we choose a_1, a_2, a_3 and b_1, b_2, b_3 such, that

$$\mathbf{PQP} = \mathbf{P} \tag{82}$$

and we obtain

$$\dot{\gamma} = \dot{\lambda} \tag{83}$$

which has the same format as in standard Drucker-Prager plasticity theory.

5.3 A Return-Mapping Algorithm

With the governing rate equations for the micro-polar elasto-plastic solid at hand, we can develop an algorithm that determines the stress increment in a finite loading step. Here, a variety of algorithms exist, but we shall only consider the Euler backward algorithm, in which the state parameters are evaluated at the end of the loading step:

$$\boldsymbol{\sigma}_{j+1} = \boldsymbol{\sigma}_0 + \mathbf{D}^{\mathrm{e}}(\Delta\boldsymbol{\epsilon} - \Delta\boldsymbol{\epsilon}^{\mathrm{p}}) \tag{84}$$

The expression for the plastic strain rate, Eq. (76) is now integrated using a single-point Euler backward rule. This results in:

$$\Delta\boldsymbol{\epsilon}^{\mathrm{p}} = \Delta\lambda \left(\frac{3\mathbf{P}\boldsymbol{\sigma}_{j+1}}{2\sqrt{\frac{3}{2}\boldsymbol{\sigma}_{j+1}^{\mathrm{T}}\mathbf{P}\boldsymbol{\sigma}_{j+1}}} + \beta\boldsymbol{\pi} \right) \tag{85}$$

so that the expression for the stress can be elaborated as:

$$\boldsymbol{\sigma}_{j+1} = \boldsymbol{\sigma}_e - \Delta\lambda \left(\frac{3\mathbf{D}^{\mathrm{e}}\mathbf{P}\boldsymbol{\sigma}_{j+1}}{2(\bar{\sigma}(\lambda_{j+1}) - \alpha\boldsymbol{\pi}^{\mathrm{T}}\boldsymbol{\sigma}_{j+1})} + \beta\mathbf{D}^{\mathrm{e}}\boldsymbol{\pi} \right) \tag{86}$$

Unfortunately, $\boldsymbol{\sigma}_{j+1}$ also enters the denominator on the right-hand side. To eliminate $\boldsymbol{\sigma}_{j+1}$ from the right-hand side of the identity we premultiply by the projection vector $\boldsymbol{\pi}$, which results in:

$$\boldsymbol{\pi}^{\mathrm{T}}\boldsymbol{\sigma}_{j+1} = \boldsymbol{\pi}^{\mathrm{T}}\boldsymbol{\sigma}_e - \Delta\lambda\beta K \tag{87}$$

with $K = \boldsymbol{\pi}^{\mathrm{T}}\mathbf{D}^{\mathrm{e}}\boldsymbol{\pi}$. For isotropic elasticity K can be identified as the bulk modulus. Substitution into Eq. (86) yields a formulation in which $\boldsymbol{\sigma}_{j+1}$ is expressed in terms of the trial stress $\boldsymbol{\sigma}_e$ and the elastic parameters:

$$\boldsymbol{\sigma}_{j+1} = \mathbf{A}^{-1}(\boldsymbol{\sigma}_e - \Delta\beta\mathbf{D}^{\mathrm{e}}\boldsymbol{\pi}) \tag{88}$$

where

$$\mathbf{A} = \mathbf{I} + \frac{3\Delta\lambda\mathbf{D}^{\mathrm{e}}\mathbf{P}}{2(\bar{\sigma}(\lambda_{j+1}) + \Delta\lambda\alpha\beta K - \alpha\boldsymbol{\pi}^{\mathrm{T}}\boldsymbol{\sigma}_e)} \tag{89}$$

Substitution in the yield condition $f(\boldsymbol{\sigma}_{j+1}, \gamma_{j+1}) = 0$ gives a non-linear equation in $\Delta\lambda$: $f(\Delta\lambda) = 0$.

5.4 Consistent Tangent Operator

For the derivation of a properly linearised set of tangential moduli we can differentiate the return map, Eq. (88), to give:

$$\dot{\boldsymbol{\sigma}} = \mathbf{H}\,(\dot{\boldsymbol{\epsilon}} - \dot{\boldsymbol{\epsilon}}^{\mathrm{p}}) \tag{90}$$

where, for Drucker-Prager plasticity:

$$\mathbf{H}^{-1} = (\mathbf{D}^{\mathrm{e}})^{-1} - \Delta\lambda\sqrt{\frac{3}{2}}\frac{\boldsymbol{\sigma}^{\mathrm{T}}\mathbf{P}\boldsymbol{\sigma}\mathbf{P} - \mathbf{P}\boldsymbol{\sigma}\boldsymbol{\sigma}^{\mathrm{T}}\mathbf{P}}{\sqrt{\boldsymbol{\sigma}^{\mathrm{T}}\mathbf{P}\boldsymbol{\sigma}}} \tag{91}$$

Since $f = f(\boldsymbol{\sigma}, \gamma)$, the consistency condition $\dot{f} = 0$ can be elaborated as:

$$\left(\frac{\partial f}{\partial \boldsymbol{\sigma}}\right)^{\mathrm{T}} \dot{\boldsymbol{\sigma}} - h\dot{\lambda} = 0 \tag{92}$$

with the hardening modulus

$$h = \frac{\partial \bar{\sigma}}{\partial \gamma} \tag{93}$$

Eqs. (90) and (92) can now be combined to give the consistent tangential stiffness relation:

$$\dot{\boldsymbol{\sigma}} = \left(\mathbf{H} - \frac{\mathbf{H}\frac{\partial g}{\partial \boldsymbol{\sigma}}\left(\frac{\partial f}{\partial \boldsymbol{\sigma}}\right)^{\mathrm{T}}\mathbf{H}}{h + \left(\frac{\partial f}{\partial \boldsymbol{\sigma}}\right)^{\mathrm{T}}\mathbf{H}\frac{\partial g}{\partial \boldsymbol{\sigma}}}\right)\dot{\boldsymbol{\epsilon}} \tag{94}$$

A deficiency of the Cosserat plasticity model is that it is only effective when the local rotations are mobilised, i.e. for mode-II failure.

6 Non-Local and Gradient Plasticity

6.1 Non-Local Plasticity

Alternatively, Bažant and Lin (1988) have suggested to average $\dot{\gamma}$ for a standard continuum, such that:

$$\dot{\bar{\gamma}}(\mathbf{x}) = \frac{1}{\Psi(\mathbf{x})}\int_V \psi(\mathbf{y}, \mathbf{x})\dot{\gamma}(\mathbf{y})\mathrm{d}V \tag{95}$$

with $V_r(\mathbf{x}) = \int g(\mathbf{s} - \mathbf{x})\mathrm{d}V$ and $g(\mathbf{s})$ a weighting function, for which the error function is usually substituted, and to make f dependent on $\bar{\gamma}$ instead of on γ:

$$f = f(\boldsymbol{\sigma}, \bar{\gamma}) \tag{96}$$

Alternatively, one can first average the plastic strain rate tensor $\dot{\boldsymbol{\epsilon}}^{\mathrm{p}}$ and then form $\dot{\bar{\gamma}}$. Numerical experience indicates that the differences between both approaches are marginal. Either approach can lead to a set of rate equations that remains elliptic after the onset of localisation. This holds true for mode-I type failure mechanisms (decohesion) and mode-II type failures (slip).

A disadvantage that adheres to non-local plasticity is the fact that the consistency condition, i.e. $\dot{f} = 0$, results in an integro-differential equation instead of in an algebraic equation that can be solved locally:

$$\left(\frac{\partial f}{\partial \boldsymbol{\sigma}}\right)^{\mathrm{T}} \dot{\boldsymbol{\sigma}} - \frac{h}{\Psi} \int_V \psi(\mathbf{y}, \mathbf{x}) \dot{\gamma}(\mathbf{y}) \mathrm{d}V = 0 \tag{97}$$

where it is implied that $\Psi = \Psi(\mathbf{x})$, $\dot{\boldsymbol{\sigma}} = \dot{\boldsymbol{\sigma}}(\mathbf{x})$ etc. Using the elasto-plastic decomposition, Eq. (65), the flow rule, Eq. (75), and the strain-hardening hypothesis, Eq. (77), we can rework this identity as:

$$\dot{\lambda} = \dot{\lambda}_{\mathrm{local}} - \frac{h}{\Psi \left(\frac{\partial f}{\partial \boldsymbol{\sigma}}\right)^{\mathrm{T}} \mathbf{D}^{\mathrm{e}} \frac{\partial g}{\partial \boldsymbol{\sigma}}} \int_V \psi(\mathbf{y}, \mathbf{x}) \dot{\lambda}(\mathbf{y}) \varphi(\mathbf{y}) \mathrm{d}V \tag{98}$$

with

$$\dot{\lambda}_{\mathrm{local}} = \frac{\left(\frac{\partial f}{\partial \boldsymbol{\sigma}}\right)^{\mathrm{T}} \mathbf{D}^{\mathrm{e}} \dot{\boldsymbol{\epsilon}}}{\left(\frac{\partial f}{\partial \boldsymbol{\sigma}}\right)^{\mathrm{T}} \mathbf{D}^{\mathrm{e}} \frac{\partial g}{\partial \boldsymbol{\sigma}}} \tag{99}$$

and

$$\varphi = \sqrt{\frac{2}{3} \left(\frac{\partial g}{\partial \boldsymbol{\sigma}}\right)^{\mathrm{T}} \frac{\partial g}{\partial \boldsymbol{\sigma}}} \tag{100}$$

Next, we consider a one-dimensional continuum for simplicity and we approximate the integral by a finite sum:

$$\dot{\lambda}_i = (\dot{\lambda}_{\mathrm{local}})_i - \frac{h}{\Psi \left(\frac{\partial f}{\partial \boldsymbol{\sigma}}\right)^{\mathrm{T}} \mathbf{D}^{\mathrm{e}} \frac{\partial g}{\partial \boldsymbol{\sigma}}} \sum_{j=0}^{n_i} w_j \psi(y_j, x_i) \dot{\lambda}(y_j) \varphi(y_j) \tag{101}$$

with w_j a weight factor. To obtain a proper solution we must carry out an iterative procedure within each global equilibrium iteration:

$$\dot{\lambda}_i = (\dot{\lambda}_{\mathrm{local}})_i - \frac{h}{\Psi \left(\frac{\partial f}{\partial \boldsymbol{\sigma}}\right)^{\mathrm{T}} \mathbf{D}^{\mathrm{e}} \frac{\partial g}{\partial \boldsymbol{\sigma}}} \sum_{j=0}^{n_i} w_j \psi(y_j, x_i) \dot{\lambda}^{k-1}(y_j) \varphi(y_j) \tag{102}$$

where the superscript k is the iteration counter. A simple alternative would be to carry out no iterations, so that:

$$\dot{\lambda}_i = (\dot{\lambda}_{\text{local}})_i - \frac{h}{\Psi \left(\frac{\partial f}{\partial \boldsymbol{\sigma}}\right)^{\mathrm{T}} \mathbf{D}^{\mathrm{e}} \frac{\partial g}{\partial \boldsymbol{\sigma}}} \sum_{j=0}^{n_i} w_j \psi(y_j, x_i) \dot{\lambda}_{\text{local}}(y_j) \varphi(y_j) \tag{103}$$

Such an averaging procedure has been utilised by Bažant and Lin (1988). Unfortunately, omission of an iteration loop in which $\dot{\lambda}_i$ is computed properly results in loss of satisfaction of the consistency condition, which makes the algorithm defect, especially for large loading steps.

The numerical difficulty discussed above does not occur when total stress-strain relations are employed, that is when the strain is not decomposed into elastic and plastic components. An example is the elasticity-based non-local damage model of Pijaudier-Cabot and Bažant (1987), where the averaging process can be carried out directly with respect to the strains.

6.2 Gradient plasticity

Gradient plasticity models can be derived from fully non-local models by first expanding the weight function $g(\mathbf{s})$ in a Taylor series about $\mathbf{s} = \mathbf{0}$ and then carrying out the integration. The result is given by

$$\dot{\bar{\gamma}} = \dot{\gamma} + c_1 \nabla^2 \dot{\gamma} + c_2 \nabla^4 \dot{\gamma} + \ldots \tag{104}$$

where the coefficients c_1, c_2 depend on the form of the weighting function and the dimension considered. Note that the odd derivates cancel because of the implicit assumption of isotropy. Restricting the treatment to second-order derivatives, the functional dependence on the yield function now becomes:

$$f = f(\boldsymbol{\sigma}, \gamma, \nabla^2 \gamma) \tag{105}$$

The numerical problem delineated above, which prevents an efficient use of elasto-plastic non-local models, in principle also applies to gradient plasticity models. However, gradient plasticity has the advantage that the consistency condition yields a partial differential equation instead of an integro-differential equation, namely for the yield function of Eq. (105):

$$\left(\frac{\partial f}{\partial \boldsymbol{\sigma}}\right)^{\mathrm{T}} \dot{\boldsymbol{\sigma}} - h\dot{\lambda} + c\nabla^2 \dot{\gamma} = 0 \tag{106}$$

where h and $\bar{c}$ are defined as:

$$h = -\frac{\dot{\gamma}}{\dot{\lambda}} \frac{\partial f}{\partial \gamma} \tag{107}$$

and

$$c = \frac{\partial f}{\partial \nabla^2 \gamma} \tag{108}$$

If the partial differential equation (106) is, just as the equilibrium condition, cf. Eq. (46), satisfied in a weak sense only, a set of equations results that is suitable as a starting point for large-scale finite element computations in two and three dimensions:

$$\int_V \delta \dot{\boldsymbol{\epsilon}}^{\mathrm{T}} \boldsymbol{\sigma} \mathrm{d}V = \int_S \delta \dot{\mathbf{u}}^{\mathrm{T}} \mathbf{t} \mathrm{d}S \tag{109}$$

and

$$\int_V \delta \dot{\lambda} \left(\left(\frac{\partial f}{\partial \boldsymbol{\sigma}} \right)^{\mathrm{T}} \dot{\boldsymbol{\sigma}} - h \dot{\lambda} + c \nabla^2 \dot{\gamma} \right) \mathrm{d}V = 0 \tag{110}$$

Together with the kinematic relations and the elastic stress-strain relation, Eq. (66), which are both satisfied in a pointwise manner, this set of equations define the elasto-plastic rate boundary value problem. The fact that the consistency condition is no longer satisfied in a pointwise manner marks a departure from return-mapping algorithms that are used in standard plasticity and in Cosserat plasticity. Now, the plastic multiplier $\dot{\lambda}$ is considered as a fundamental unknown and has a role similar to that of the displacements. It is solved for at global level together with the displacement degrees-of-freedom.

The displacement field $\mathbf{u}$ and the field of plastic multipliers λ can be discretized to nodal variables $\mathbf{a}$ and $\boldsymbol{\Lambda}$:

$$\mathbf{u} = \mathbf{H}\mathbf{a} \ , \ \ \lambda = \mathbf{h}^{\mathrm{T}} \boldsymbol{\lambda} \tag{111}$$

Use of a Bubnov-Galerkin approach and linearising then leads to the following set of equations:

$$\begin{bmatrix} \mathbf{K}_{\mathrm{aa}} & \mathbf{K}_{\mathrm{a}\boldsymbol{\lambda}} \\ \mathbf{K}_{\mathrm{a}\boldsymbol{\lambda}}^{\mathrm{T}} & \mathbf{K}_{\boldsymbol{\lambda}\boldsymbol{\lambda}} \end{bmatrix} \begin{pmatrix} \mathrm{d}\mathbf{a} \\ \mathrm{d}\boldsymbol{\lambda} \end{pmatrix} = \begin{pmatrix} \mathbf{f}_{\mathrm{ext}}^{\mathrm{a}} - \mathbf{f}_{\mathrm{int}}^{\mathrm{a}} \\ \mathbf{0} \end{pmatrix} \tag{112}$$

where

$$\mathbf{K}_{\mathrm{aa}} = \int_V \mathbf{B}^{\mathrm{T}} \mathbf{D}^{\mathrm{e}} \mathbf{B} \mathrm{d}V \tag{113}$$

$$\mathbf{K}_{\mathrm{a}\boldsymbol{\lambda}} = -\int_V \mathbf{B}^{\mathrm{T}} \mathbf{D}^{\mathrm{e}} \frac{\partial f}{\partial \boldsymbol{\sigma}} \mathbf{h}^{\mathrm{T}} \mathrm{d}V \tag{114}$$

$$\mathbf{K}_{\boldsymbol{\lambda}\boldsymbol{\lambda}} = \int_V \left[\left(h + \left(\frac{\partial f}{\partial \boldsymbol{\sigma}} \right)^{\mathrm{T}} \mathbf{D}^{\mathrm{e}} \frac{\partial f}{\partial \boldsymbol{\sigma}} \right) \mathbf{h}\mathbf{h}^{\mathrm{T}} - c\mathbf{h}\nabla^2 \mathbf{h}^{\mathrm{T}} \right] \mathrm{d}V \tag{115}$$

and $\mathbf{f}_{\text{ext}}$ the external force vector. In the preceding $\mathbf{h}^{\mathrm{T}} = (h_1, \ldots, h_n)$ is the vector that contains the interpolation polynomials for the plastic multiplier and $\mathbf{p}^{\mathrm{T}} = (\nabla^2 h_1, \ldots, \nabla^2 h_n)$. The detailed derivation of these equations and the finite elements that have been constructed on the basis of them are described in de Borst and Mühlhaus (1992); de Borst and Pamin (1996).

An unpleasant property of Eq. (112) is the unsymmetry that enters through $\mathbf{K}_{\lambda\lambda}$. For the pure rate problem $\mathbf{K}_{\lambda\lambda}$ can be symmetrised. Introducing $\mathbf{q}^{\mathrm{T}} = (\nabla h_1, \ldots, \nabla h_n)$ and using Green's theorem we obtain

$$-\mathbf{h}\nabla^2\mathbf{h}^{\mathrm{T}} \rightarrow \nabla\mathbf{h}\nabla\mathbf{h}^{\mathrm{T}} \tag{116}$$

and the non-standard boundary conditions at the elasto-plastic boundary S_λ: $\delta\dot{\lambda} = 0$ or $(\nabla\dot{\lambda})^{\mathrm{T}}\mathbf{n}_\lambda = 0$, with $\mathbf{n}_\lambda$ the outward normal at S_λ.

Bibliography

Z. P. Bažant and F.B. Lin. Non-local yield limit degradation. *International Journal for Numerical Methods in Engineering*, 26:1805–1823, 1988.

A. Benallal, R. Billardon, and G. Geymonat. Some mathematical aspects of the damage softening rate problem. In J. Mazars and Z. P. Bažant, editors, *Cracking and Damage*, pages 247–258, Amsterdam, 1988. Elsevier.

R. de Borst and H. B. Mühlhaus. Gradient-dependent plasticity: formulation and algorithmic aspects. *International Journal for Numerical Methods in Engineering*, 35:521–539, 1992.

R. de Borst and J. Pamin. Some novel developments in finite element procedures for gradient-dependent plasticity. *International Journal for Numerical Methods in Engineering*, 39:2477–2505, 1996.

R. de Borst, A. Benallal, and O. M. Heeres. A gradient-enhanced damage approach to fracture. *Journal de Physique IV*, C6:491–502, 1996.

H. P. J. de Vree, W. A. M. Brekelmans, and M. A. J. van Gils. Comparison of nonlocal approaches in continuum damage mechanics. *Computers and Structures*, 55: 581–588, 1995.

R. Hill. A general theory of uniqueness and stability in elastic-plastic solids. *Journal of the Mechanics and Physics of Solids*, 6:236–249, 1958.

R. Hill. Acceleration waves in solid. *Journal of the Mechanics and Physics of Solids*, 10:1–16, 1962.

W. T. Koiter. On the thermodynamic background of elastic stability theory. In *Problems of Hydrodynamics and Continuum Mechanics*, pages 423–433. SIAM, 1969.

J. Lemaitre and J. L. Chaboche. *Mechanics of Solid Materials*. Cambridge University Press, Cambridge, UK, 1990.

G. Maier and T. Hueckel. Nonassociated and coupled flow rules of elastoplasticity for rock-like materials. *International Journal of Rock Mechanics and Mining Sciences & Geomechanical Abstracts*, 16: 77–92, 1979.

J. Mazars and G. Pijaudier-Cabot. Continuum damage theory – application to concrete. *ASCE Journal of Engineering Mechanics*, 115:345–365, 1989.

R. H. J. Peerlings, R. de Borst, W. A. M. Brekelmans, and H. P. J. de Vree. Gradient-enhanced damage for quasi-brittle materials. *International Journal for Numerical Methods in Engineering*, 39:3391–3403, 1996.

R. H. J. Peerlings, M. G. D. Geers, R. de Borst, and W. A. M. Brekelmans. A critical comparison of nonlocal and gradient-enhanced softening continua. *International Journal of Solids and Structures*, 38:7723–7746, 2001.

G. Pijaudier-Cabot and Z. P. Bažant. Nonlocal damage theory. *ASCE Journal of Engineering Mechanics*, 113:1512–1533, 1987.

G. Pijaudier-Cabot and A. Huerta. Finite element analysis of bifurcation in nonlocal strain softening solids. *Computer Methods in Applied Mechanics and Engineering*, 90:905–919, 1991.

J. W. Rudnicki and J. R. Rice. Conditions for the localization of deformation in pressure sensitive dilatant materials. *Journal of the Mechanics and Physics of Solids*, 23:371–394, 1974.

J. C. Simo and J. W. Ju. Strain- and stress-based continuum damage formulations – Part I: Formulation – Part II: Computational aspects. *International Journal of Solids and Structures*, 23: 821–869, 1987.

I. Vardoulakis and J. Sulem. *Bifurcation Analysis in Geomechanics*. Blackie, London, UK, 1995.